This study solves the relevant problem of selecting an optimal switching and measurement circuit for the problems of reconstruction of the field of change in the conductivity in a biological object.

Based on an analysis of publications in the area of construction of the hardware part of the EIT devices, the main types of the systems were identified: sequential, parallel, and mixed. Because of the low cost, sequential architecture became most common.

Due to the low level of a useful signal in the study of lung ventilation, the differential measurement circuit, which enables amplification of a difference signal, is considered optimal. A difference signal changes significantly as it moves away from injecting electrodes, so the optimal use of the analog-to-digital converter scale requires a change in the amplification coefficient during the collection of measurement information. A measurement circuit with an adaptive amplification coefficient was proposed. The optimal amplification coefficient is determined by the results of test measurements. A block diagram for the implementation of the proposed algorithm was developed.

A circuit for switching the injecting and measuring electrodes, allowing the injection and measurement between any pair of electrodes, was proposed. Theoretical analysis of the impact of switch parameters was carried out. The analysis revealed that the main parameters influencing the metrological characteristics are the resistance of the open channel and its spread.

As a result of mathematical modeling of the circuit of substitution of injection and measurement channels, it was determined that channel resistance and its spread for typical switches results in a relative error in measurements of potentials of no more than 0.2 %

Keywords: electric impedance tomography, image reconstruction, medical visualization, conductivity distribution, measurement, switcher

UDC 617-7, 004.942
DOI: 10.15587/1729-4061.2020.210776

DEVELOPMENT OF SWITCHING AND MEASUREMENT CIRCUITS FOR PROBLEMS OF ELECTRIC IMPEDANCE TOMOGRAPHY

A. Kucher
PhD, Associate Professor*
E-mail: a.kucher@npi-tu.ru
N. Narakidze
PhD, Associate Professor*
E-mail: ndaz@mail.ru
P. Tjaglicova *
E-mail: polina.vladimirovna.t@gmail.com
M. Filonova
Research Assistant*
E-mail: filonovamaryana@yandex.ru
*Department of Information and Measuring Systems and Technologies
Federal State Budget Educational Institution of Higher Education "Platov South-Russian State Polytechnic University (NPI)"
Prosveshcheniya str., 132, Novocherkassk, Russian Federation, 346428

Received date 27.07.2020
Accepted date 21.08.2020
Published date 31.08.2020

1. Introduction

Electric impedance tomography (EIT) is a method for obtaining and visualizing the data on conductivity distribution in the volume of an examined object. The promising direction of the EIT is the three-dimensional EIT (3D EIT), which makes it possible to obtain information on the parameters of the field of conductivity of the internal structures of the object under study by the totality of two-dimensional tomographic slices.

The EIT concept involves laying electrodes on the object of examination (OE), sending a signal of injected current to two of them, and measuring the difference of the potentials on the rest of them. Under the "Sheffield protocol" of injection and measurement, in order to obtain one measurement frame, the difference of potentials is measured on all pairs of neighboring electrodes, as shown in Fig. 1. When conducting the examination with the use of electric impedance tomography, accurate measurement of electrical parameters of the examination object is the most important task. Given that the frequency of the injected current can reach the values of several megahertz [1], there are high requirements for the rapid action of the measurement circuit.

The general block diagram of measurement unit operation is shown in Fig. 2.

As it can be seen from the diagram, a measuring signal in the form of electrical potentials φ_i or their difference $\Delta\varphi_i$ after the necessary switching is increased to the specified values and then is measured.

Its conductivity field σ in the OE is reconstructed (or changed) based on the measured values of potentials φ_i or their difference $\Delta\varphi_i$ and prior information about the object.

Thus, the quality of measurement information has a significant impact on the results of the reconstruction of a change in the conductivity field of an examined object. Therefore, the choice of the optimal switching and measurement circuit is a relevant task.

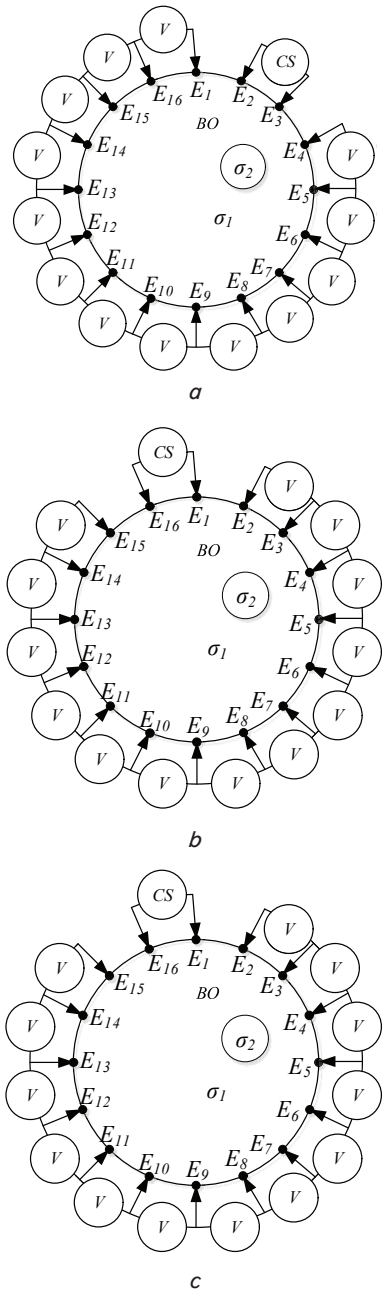

Fig. 1. Circuit of connection of injecting and measuring electrodes during the EIT examination: *a* — configuration of injecting electrodes No. 1; *b* — configuration of injecting electrodes No. 2; *c* — configuration of injecting electrodes No. 16

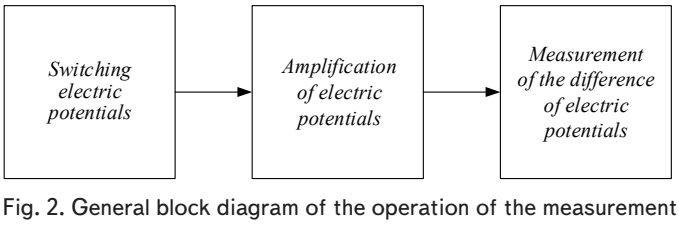

Fig. 2. General block diagram of the operation of the measurement system of electrical impedance tomography

2. Literature review and problem statement

In general, the EIT systems can be divided [2] into devices with:

– sequential architecture,
– parallel architecture,
– mixed architecture.

Sequential architecture implies the use of one injection channel and one measurement channel. The injection and measurement channels are connected to the given electrodes using analog switches. On the one hand, outside units with unstable characteristics appear in the measurement. The time of information collection increases significantly due to the impossibility of parallel information reading from more than a couple of electrodes. On the other hand, there is no need to calibrate multiple sources of current or measuring tracts, and thus the total cost of the device decreases.

Parallel architecture implies one injection and measurement channel for each pair of electrodes. This architecture makes it possible to simultaneously record the potentials between all necessary electrodes, significantly reducing the time of information collection, and to inject current to all electrodes simultaneously. However, the cost of the device increases significantly. The problems of harmonization of metrological characteristics of measurement and injection channels appear as well.

The mixed structure implies a compromise between the parallel and the sequential architecture. Take, for example, the sequential injection architecture and the parallel architecture of recording potentials. It is also possible to implement the parallel architecture on a group of electrodes. Thus, for example, the parallel architecture with four measurement channels will make it possible to record differences of potentials between 8 electrodes simultaneously. This approach to a 16-electrode system will reduce data collection time by 4 times compared to the sequential architecture.

There are many publications on the development of electric impedance tomography devices [3–10]. Paper [3] addresses the development of a low-cost implementation of the non-disruptive control system based on the EIT. The device is based on the Arduino UNO board and the EIT board, which combines a probe signal generator and switches. Paper [4] tackles the development of an electrode system for the EIT and contains a description of the portable EIT system. Paper [5] includes a description of a data collection and transmission device based on the Arduino 2560 board with external switches and measurement of potentials relative to the common point. However, in this paper, the questions of assessing the accuracy of the chosen approach remained unresolved. Paper [6] describes the process of the development of a portable EIT system to monitor cardiovascular system activity. However, the focus is on the arrangement of a wireless connection of a device with a smartphone. Article [7] contains a description of a test stand to study the applicability of EIT in predicting the behavior of electrically conductive structures. The choice of the structure of the test stand is not substantiated. Article [8] explores the process of developing an EIT device with mixed architecture – 16 measuring channels and one multiplexing injection channel. The problems of the impact of the chosen architecture on measurement results did not receive due attention. Paper [9] reports a study into the influence of the structure of a measuring channel on the phase component of a measuring signal. Article [10] addresses the development of active measuring electrodes. Most of the devices [3–7] are constructed based on the sequential architecture. Analysis of publications on this topic has shown that little attention

is paid to the issues of development of hardware architecture. The issues of substantiation of the architecture of the measuring tract have not been dealt with within the past 10 years. Developers choose the most common structure for its ease of implementation and low cost of the hardware part. The authors mainly assess the quality of the device operation by the results of reconstruction. At the same time, assessment usually boils down to the estimation of a change in the "phantom" conductivity or to the estimation of a change in the conductivity of the thoracic cavity. These examination objects have a high change in conductivity, which decreases the requirements to the hardware part. At the same time, changes in the conductivity of thoracic tissues from filling with blood are often not recorded due to the limitations of the most common decisions. The issues of design of measurement and switching circuits in the EIT received little attention. Thus, it is necessary to carry out research into the architecture of the switching and measurement circuit on the result of recording the potentials in the EIT.

3. The aim and objectives of the study

The aim of this research is to identify the optimal structure of the measurement channel for optimal use of the ADC scale in EIT devices and to assess the impact of the architecture of a switch circuit on the result of recording the potentials in the EIT devices.

To accomplish the aim, the following tasks have been set:

– to determine the basic measurement circuits in the EIT and the principles of their operation;

– to develop a switch circuit, the principles of its functioning and to assess the impact of the circuit on the operation of injection and measurement systems;

– to assess experimentally the impact of selected circuit technical solutions on measurement error.

4. Basic measurement circuits in EIT and the principles of their functioning

To solve the problem of measurement of electric potentials from the surface of an examined object, several approaches to the construction of circuits of measurement data collection are applied in the EIT problems. One of them involves measuring the electric potential on one electrode relative to a common point [11]. The block diagram of such a solution is shown in Fig. 3.

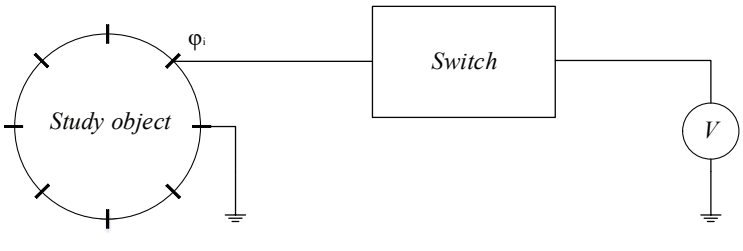

Fig. 3. Block diagram of hardware for measurement of electric potential relative to a common point

The block diagram of the measurement algorithm using this approach is shown in Fig. 4. In this case, n potentials φ_i (i=1...n) are recorded, and $\Delta\varphi_i$ is computed from the formula:

$\Delta\varphi_i=\varphi_{i+1}-\varphi_i$.

Electrodes are sorted out by order, that is, the variable "electrode number" is incremented in each iteration.

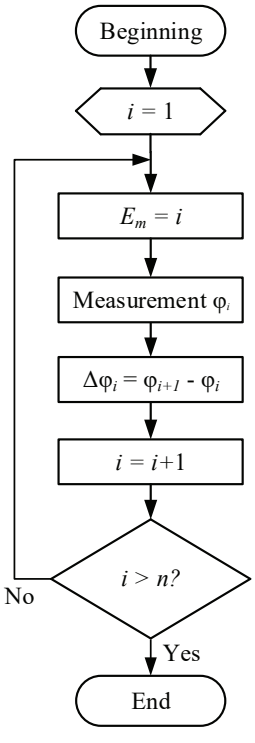

Fig. 4. Block diagram of the algorithm of measurement of electrical potentials relative to a common point

As the block diagram shows, at one moment, potential φ_i is measured on one electrode E_m. $\Delta\varphi_i$ between neighboring E_m, E_{m+1} is computed in a separate unit.

The main advantage of this approach is the ease of implementation, which requires a minimum number of switches. At the same time, the presented circuit has a serious disadvantage. The level of $\Delta\varphi_i$ during the examination of biological objects makes up unities or dozens of microvolts, and the level of φ_i is unities of volts. Thus, when measuring φ_i with high accuracy, the measurement error will be at the level of or above the values of $\Delta\varphi_i$.

When measuring close values of φ_i and φ_{i+1}, a device must have a range of input values of $U_{\max}$, that allow measuring φ_i, and at the same time, the resolution that will make it possible to compute $\Delta\varphi_i$ with a permissible error.

There is also a known circuit, in which the difference of potentials $\Delta\varphi_i$ between two electrodes is measured directly; the block diagram of such a solution is shown in Fig. 5.

The accuracy of this approach to measuring $\Delta\varphi_i$ is much higher, as the difference of potentials $\Delta\varphi_i=\varphi_{i+1}-\varphi_i$ can have a comparable level with the range of input values of the measuring device. Thus, the considered approach makes it possible to perform measurement with higher accuracy. The disadvantages of this approach include doubling the number of analog multiplexers needed to implement the approach described. In addition, low levels of $\Delta\varphi_i$ can require a circuit of differential signal amplification. Despite the more complex implementation of the considered

approach, the benefits in the form of high-precision $\Delta\varphi_i$ measurement make it possible to separate this approach as more preferable for practical implementation.

Consider the existing approaches to the construction of circuits of differential signal amplification.

The traditional approach to the construction of amplification circuits involves the use of a differential amplifier with a fixed amplification coefficient K_u. An example of the implementation of this approach is shown in Fig. 5.

The implementation represented in Fig. 5 shows that the circuit ensures subtraction of φ_i from φ_{i+1}, that is, obtaining the sought for $\Delta\varphi_i$. In addition, $\Delta\varphi_i$ is amplified to U_{out}, necessary to record a measuring signal with the use of the analog-to-digital converter (ADC):

$$U_{out} = \Delta\varphi_i \cdot K_U,$$

$$K_U = \frac{R_2}{R_3} = \frac{R_4}{R_1}.$$

As previously stated, the described approach ensures fixed K_U. However, it should be taken into consideration that for high values of $\Delta\varphi_i$, the value of U_{out} may exceed $U_{\max}$ of the ADC. This can lead to erroneous measurement results and possible failure of the ADC.

To prevent the occurrence of such situations, a manual change of K_u by changing the nominal of feedback resistors R_2 and R_4 is a possible solution. However, there arises a problem of conducting research in the automatic mode, that is, without the operator's intervention.

To solve the specified problem, it is necessary to replace, in the block diagram shown in Fig. 6, an amplifier with fixed K_U, assigned by discrete feedback resistors, with an amplifier with modified K_U. So-called amplifiers with programmable amplification coefficient (PA) are used for these purposes. It is also necessary to introduce feedback in order to realize effectively the capabilities of a tool such as a PA. In this regard, it is proposed to introduce a control unit, which, based on the digital ADC-generated code, assigns K_U for the PA.

An example of the implementation of this approach is shown in Fig. 7.

The proposed approach also requires the development of an algorithm for the functioning of the control unit. The block diagram of the developed algorithm for the considered solution is presented in Fig. 8.

As the block-diagram presented in Fig 8 shows, the minimal value K_U=1 is chosen for primary measurement. Based on the results of primary measurement, the K_U value is selected so that product of K_U and $\Delta\varphi_i$ should not exceed the $U_{\max}$: value:

$$K_U \rightarrow \frac{U_{\max}}{\Delta\varphi_i}.$$

The result is a final measurement of $\Delta\varphi_i$ using the chosen K_U.

The developed algorithm together with the proposed approach makes it possible to implement an adaptive system for measuring a wide range of $\Delta\varphi_i$ values with minimizing the additive error of ADC without risk of exceeding $U_{\max}$ [12].

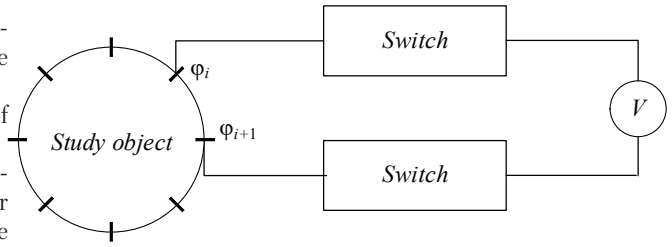

Fig. 5. Block diagram of hardware for differential measurement of $\Delta\varphi_i$

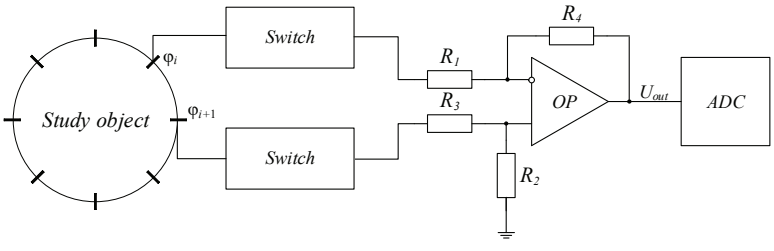

Fig. 6. Implementation of an approach to the construction of a circuit of a differential amplifier with a fixed amplification coefficient K_u

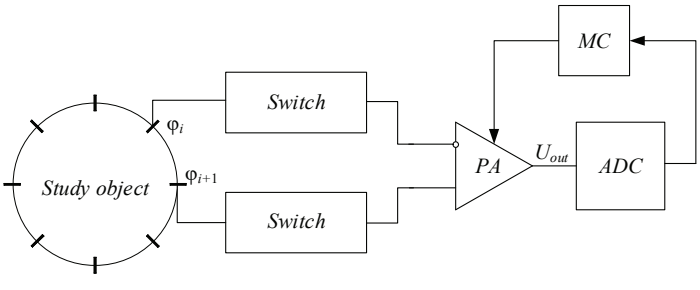

Fig. 7. Implementation of the approach to the construction of the circuit of a differential amplifier with a changeable amplification coefficient K_u

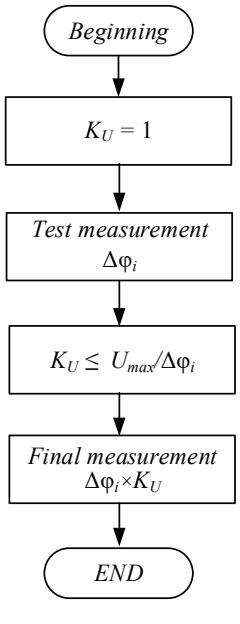

Fig. 8. Block-diagram of the algorithm of measurement of $\Delta\varphi_i$ with the use of PA

As part of this work, it is also necessary to form requirements for the most important component of the measuring

circuit – the analog-to-digital converter. As previously stated, the most important characteristics of the measuring circuit are the accuracy of measurement and its promptness.

Measurement accuracy $\Delta\varphi_i$ is determined by the class n of the ADC:

$$1LSB = \frac{U_{\max}}{2^n},$$

where LSB is the voltage value for the least significant (junior) bit. Obviously, for accurate measurement of $\Delta\varphi_i$, the value of LSB should be much less than $\Delta\varphi$:

$$1LSB \ll \Delta\varphi_i.$$

The LSB value is a parameter that determines the additive error of the ADC as well [12].

The rapid operation of the ADC is determined by the discretization frequency f_d. According to the Shannon-Nyquist theorem, any function consisting of frequencies from 0 to f can be restored [13], if the following condition is met:

$$f_d > 2 \cdot f,$$

Thus, when choosing the ADC, it is necessary to be guided by preliminary information about the minimum amplitude of a measuring signal and its maximum frequency.

5. Development of the switching circuit, its operation principles and assessment of the impact on the operation of injection and measurement systems

As can be seen from the block diagram presented in Fig. 2, the same electrodes should be connected to different sources and receivers of a signal, which implies the high flexibility of a switching circuit.

Fig. 9 shows the block diagram of the switching unit of injection and measurement channels used in the EIT problems. According to the presented diagram, the microcontroller MC performs the functions of control over injection and measurement channels of the device. To do this, the MC sends digital codes D to address buses to each of the switches (address buses are shown by the dotted line). A pair of switches is connected to the current source CS, the pair is connected to the measurement circuit V (these connections are marked by a continuous line).

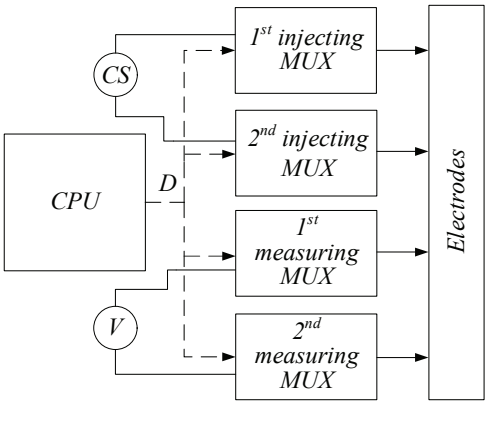

Fig. 9. Block diagram of the switching unit of injecting and measuring signals of the EIT device

Analog multiplexers are used as switches for each of the injecting and measuring channels; the number of channels in each multiplexer must be not less than the number of electrodes n.

According to the circuit of connection of injecting and measuring channel, shown in Fig. 1, and the block diagram, shown in Fig. 7, the following block diagram of the channel switching algorithm for the MC of the EIT device, shown in Fig. 10, was developed.

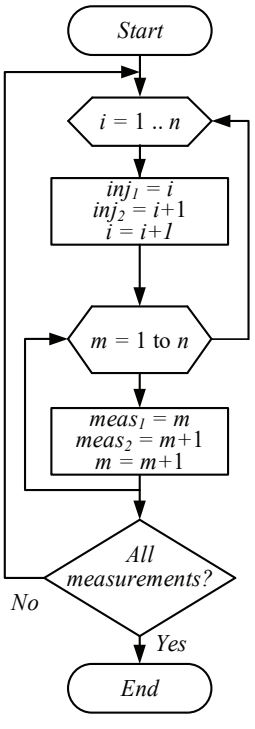

Fig 10. Block diagram of the algorithm of switching electrodes during the EIT examination

According to the shown block-diagram, injecting electrodes i and i+1 are connected to channels inj_1 and inj_2. Measuring electrodes m and m+1 are connected to channels $meas_1$ and $meas_2$. The measurement process continues until at inj_1=i and inj_2=i+1 all measuring electrodes m=1..n are asked.

When switching injecting channels inj_1 and inj_2, the measurement process is repeated until all injecting electrodes i=n are connected.

When using analog multiplexers, it is important to assess their impact on the operational and metrological characteristics of the entire device. Important characteristics of the analog multiplexer are the resistance of open channel R_{mux} and the spread of the values of this resistance between channels R_{match}. We will assess the impact of these parameters on the EIT examination process.

As it is known [14], the simplest equivalent electrical circuit for substitution of a biological object can be presented as a section of an electrical circuit consisting of two elements: active resistance RE and capacity CE connected in parallel (Fig. 11).

For such an equivalent circuit with the parallel connection of the elements, impedance Z can be determined from the following expression [14]:

$$Z = \frac{R_E \cdot jX_{C_E}}{R_E + jX_{C_E}},$$

where X_{C_E} is the resistance of electric capacity to AC:

$$X_{C_E} = \frac{1}{2\pi \cdot f \cdot C},$$

where f is the frequency of injecting current.

Taking into consideration the accepted equivalent circuit of the biological object, we will construct an equivalent circuit of the measuring channel of the EIT device connected to the object of examination (Fig. 12).

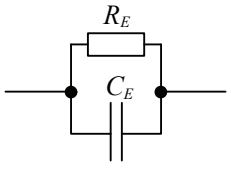

Fig. 11. Equivalent electrical circuit of substitution of a biological object

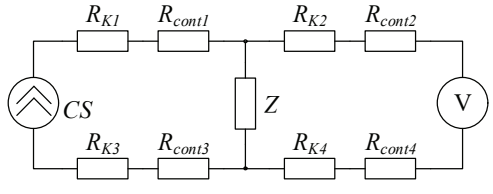

Fig. 12. Equivalent electrical circuit of the measuring channel of the EIT device connected to a biological object

Consider the section of the circuit, where the source of the injecting signal CS is connected to the object of examination Z through K1 and K3 switches with channel resistance R_{K1} and R_{K2}, respectively. In addition, in the circuit, there is contact resistance of electrodes R_{cont}. Given that CS is the current source [15], the value of output current I does not depend on load resistance. Therefore, we can conclude that current I, which also passes through Z, does not depend on the values of R_K and R_{cont} either. At the same time, the voltage of this circuit section U_{CS}, which can be described by the following formula

$$U = I \cdot \left(R_{K1} + R_{K3} + R_{cont1} + R_{cont3} + Z\right),$$

should not exceed the value of $U_{\max}$, which can be developed by *CS:*

$$U \leq U_{\max}.$$

Thus, R_K and R_{cont} do no influence current I, passing through a biological object with impedance Z. However, the use of the switches decreases the maximum value of Z in the injection circuit due to the limitation of the maximum output voltage of CS $U_{\max}$.

Thus, when designing the EIT device, it is necessary to select analog multiplexors with a minimum possible value of R_K. Level R_{cont}, in this case, is not important.

Similarly, consider the circuit section, where measurement device V is connected to the object of examination Z to measure U_Z. Because input resistance is high (infinitely high for ideal V), the measured value of U_Z does not depend on the values of R_K for each multiplexer of the measurement circuit either. Given the foregoing, the requirements for minimal possible values of R_K for switches of measuring circuits are not compulsory.

Thus, the conducted study shows the lack of influence of the main parameters of analog multiplexers on the metrological characteristics of the EIT device. At the same time, the values of R_K of the switches of the circuit of injecting current limit the maximal level of load on the CS due to the limitation of the maximum output CS voltage $U_{\max}$. That is why analog multiplexers for injecting channels should be chosen with minimal possible resistance of open channel R_K.

6. Experimental studies of the switching and measurement circuit

Experimental research is needed to verify the results of the study of the impact of the main parameters of analog multiplexers on the metrological characteristics of the EIT device. Experimental studies of the switching and measurement circuit were carried out in the MicroCap 12 package [16].

In order to study the effect of the resistance of open channel R_K of analog multiplexers on the metrological characteristics of the EIT device, we conducted a simulation of the electric circuit, shown in Fig. 12. The simulation was carried out in the MicroCap package. When using electrode gel for the ECG, the R_{cont} decreases significantly. Due to this circumstance, R_{cont} was not taken into consideration in the simulation. Resistances R_{match} were added to study the effect of the spread of multiplexer characteristics.

For R_{mux}, a typical value of resistance of the open channel for commonly available 16-channel multiplexers were selected, R_{mux}=50 ohm. The range of changing of *Rcont* was selected from 0 to 20 ohm, that is, 40 % of R_K. This "deterioration" of the characteristics of a multiplexer will make it possible to visualize the measurement error in case it occurs. The typical value of *Rcont* for common multiplexers does not exceed 10 %.

Parallel connection R_H=100 ohm and C_H=200 pF [14] were chosen as a load. The choice of the value of R_{load}, close to R_{mux}, will also make it possible to detect more effectively the measurement error, should it occur.

We selected the frequency of current source If_I=100 kHz, current strength I=5 mA. To model the measurement circuit, we selected a differential amplifier on operation amplifier *AD*8253 [17], connected to resistance R_{ADC}, imitating input resistance of the analog-to-digital converter.

The circuit of the switching and measurement unit, modeled in the MicroCap package, is shown in Fig. 13, *a*. Parameters of the study are shown in Fig. 13, *b*.

The results of the modeling are shown in Fig. 14.

As can be seen from the diagram shown in Fig. 14, the shape of the curve of the changed voltage *v(RADC)* coincides with the curve of current from the outlet of current source *i*(*I*1). In this case, the maximum value $v_{\max}(R_{\text{ADC}})$, corresponding to R_{match}=20 Ohm, is 498.007 mV, while at R_{match} =0 ohm, $v_{\min}(R_{\text{ADC}})$=497.029 mV.

Calculate the relative error δ of values of the amplitude of the changed voltage $v(R_{\text{ADC}})$, which is evaluated from the following formula:

$$\delta = \frac{\left|\mathrm{v}_{\min}\left(\mathrm{R}_{\text{ADC}}\right) - \mathrm{v}_{\max}\left(\mathrm{R}_{\text{ADC}}\right)\right|}{\mathrm{v}_{\min}\left(\mathrm{R}_{\text{ADC}}\right)} \cdot 100\,\%.$$

Error δ $v(RADC)$ is

$$\delta = \frac{|497{,}029 - 498{,}007|}{498{,}007} \cdot 100\,\% = -0{,}196\,\%.$$

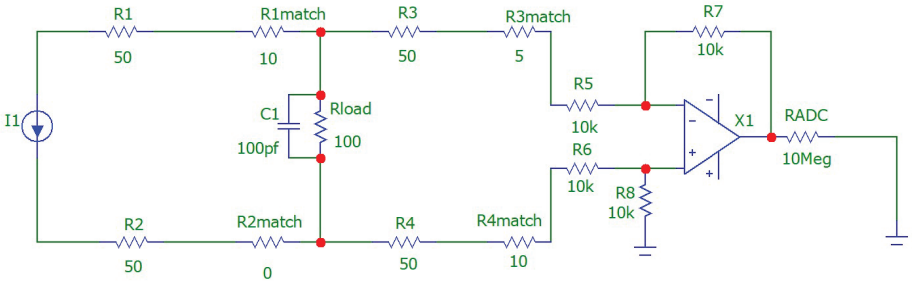

Fig. 13. Model of an equivalent electric circuit of the injecting and measuring channel in MicroCap package

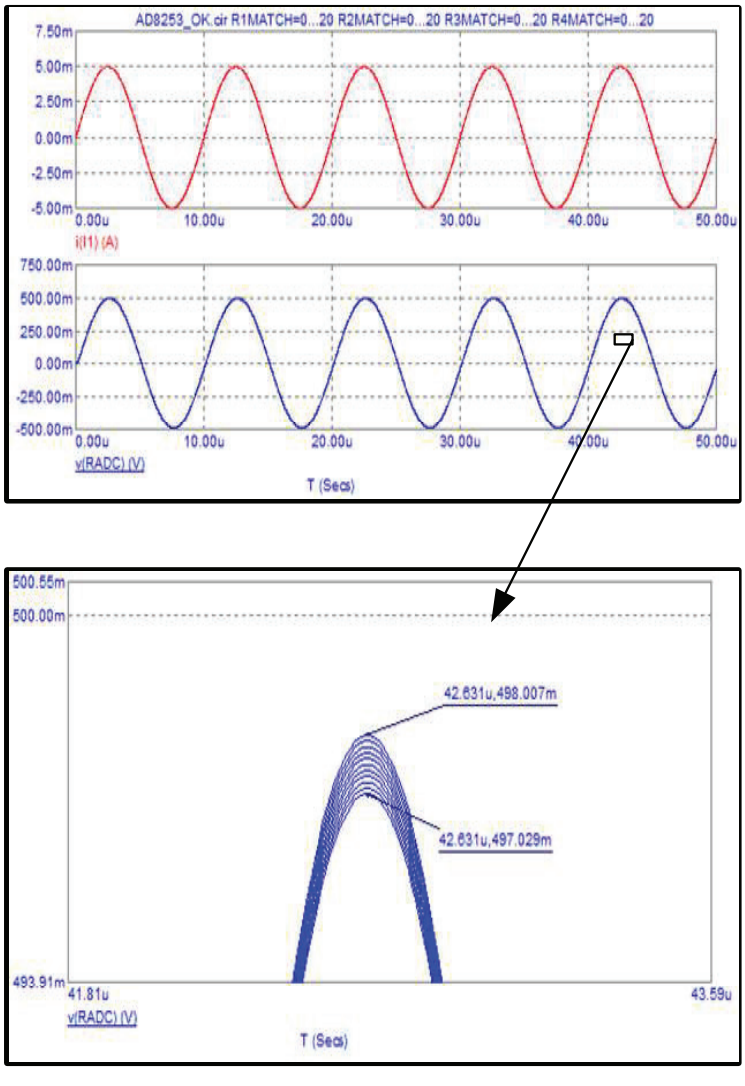

Fig. 14. Results of modeling in MicroCap package

Thus, analysis of data $\delta\, v(R_{ADC})$, obtained as a result of modeling, reveals that discrepancy δ between values of $v_{min}(R_{ADC})$ and $v_{max}\,(R_{ADC})$ does not exceed 0.2 %.

7. Discussion of the results of studying the switching and measurement architectures in the EIT

It is easier to implement the recording of potentials relative to a common point (Fig. 3). However, the specificity of the EIT of the thoracic cavity is that a useful signal is much less than the values of potentials on the surface of the thoracic cavity. In this case, the differential circuit (Fig. 5) makes it possible to distinguish a useful signal, after which it can be amplified to reduce the measurement error. The difference in potentials between injecting electrodes is much higher than the difference of potentials between non-injecting electrodes. Therefore, the use of the circuit with a fixed amplification coefficient (Fig. 6) does not make it possible to obtain acceptable metrological characteristics due to the use of a limited part of the ADC scale. The circuit of differential amplification with a programmable amplifier and the algorithm for adaptive change in the amplification coefficient were proposed. The algorithm involves conducting a test measurement to determine the optimal amplification coefficient, followed by recording the difference of potentials. Previously, these issues were not given due attention in the literature.

The proposed structural circuit of the injection and measurement switching unit (Fig. 9) makes it possible to connect the current source and the measuring device to any pair of electrodes. This circuit implements the sequential architecture of measurement and injection. The main parameters of the switching circuit influencing the operation of injection and measurement systems are resistances of switching channels (Fig. 12). These resistances do not influence the measurement system due to extremely small currents in the measuring circuit. Small currents of the measuring circuit are caused by high input resistance of the measuring amplifier. Getting resistances into the injection channel limits the maximum value of load in the injection chain. Thus, it is necessary to choose switches with minimal resistance to the open channel.

To assess the impact of resistance of the open channel of the multiplexer and its spread, a model of the circuit of substitution of the injection and measurement channel in the *MicroCAP* environment of schematic-technical modeling was developed. During the experiment, the value of resistance of the open multiplexer channel varied within nominal values. The relative error of recording potentials was assessed.

The studies of the circuit of substitution of injection and measurement channels in *MicroCAP* proved the conclusions obtained during analysis. An assessment of the impact of the spread of resistance of the open channel of the

typical analog switcher showed that the impact on the relative error of recording potentials does not exceed 0.2 %.

This paper explored the impact of the parameters of the elements of the sequential structure of the EIT devices on the error of recording potentials. The dynamic characteristics of this approach are not considered. Similar studies of parallel architecture are planned in the course of further work. The experience of developing devices for the EIT suggests that the mixed architecture – sequential injection with the parallel recording of potentials – is optimal

8. Conclusions

1. Recording potentials relative to the common point, followed by a program calculation of the difference of potentials is hardly possible in the EIT of the thoracic cavity due to the impossibility of amplification of the difference of potentials. The need for amplification is due to the small amplitude of this difference. Differential measurement with a fixed amplification coefficient due to a significant change in the level of difference of potentials at distancing from injecting electrodes makes the optimal use of the ADC scale impossible. The proposed measurement circuit with the adaptive measurement coefficient allows changing the amplification coefficient when measuring each potential on the surface of the thoracic cavity. To do this, the circuit based on a measuring amplifier with a programmable amplification coefficient was developed. The algorithm of control of the amplification coefficient is to conduct a test measurement to calculate the optimal amplification coefficient. The developed approach enables recording the differences of potentials on the surface of the thoracic cavity with the minimum admissible error for the used hardware.

2. The developed switching circuit is based on a sequential structure and makes it possible to connect the source of the current and voltage meter to any pair of electrodes on the surface of the thoracic cavity. The algorithm of the switching circuit operation implements sequential injection into neighboring pairs of electrodes with a sequential recording of the differences of potential between neighboring pairs of electrodes, which makes it possible to use one current source and one measurement circuit. The main parameters of switches that affect the operation of the injection and measurement circuit are the resistance of the open channel and its spread due to the sequential connection of a switch in the injection chain and the measurement circuit. The measurement circuit has a high resistance factor, which is why ultra-small currents flow in the measuring circuit. These currents cause a voltage drop on switches, which is less than ADC discreteness, so the impact of switches on the measurement circuit is negligible. The existence of switches in the injection circuit reduces the load capacity of the current source due to the sequential connection of the switches' resistance with the chest. However, this shortcoming can be eliminated by increasing the load capacity of the current source.

3. The developed circuit of substitution of the injection and measurement channel allowed assessing the impact of resistance of the switch channel and its spread on the error of measurement of the difference of potentials. The relative error of recording the potentials for the EIT at a variation of resistance of multiplexer channels in the nominal range did not exceed 0.2 %. Therefore, the use of analog switches in the injection and measurement circuit insignificantly decreases the metrological characteristics of the EIT device in comparison with the parallel architecture.

Acknowledgment

The research is carried out within the framework of the federal target program "Research and development in priority areas of development of the Russian scientific and technological complex for 2014–2020" with the financial support from the Ministry of Science and Higher Education (agreement No. 05.607.21.0305). Unique identifier of agreement RFMEFI60719X0305.

References

1. Pekker, Ya. S., Brazovskiy, K. S., Usov, V. N. (2004). Elektroimpedansnaya tomografiya. Tomsk: NTL, 192.
2. Brazovskiy, K. S. (2015). Metody i tekhnicheskie sredstva otsenki funktsional'nogo sostoyaniya golovnogo mozga cheloveka na osnove elektricheskikh izmereniy. Tomsk. Available at: http://earchive.tpu.ru/bitstream/11683/30581/1/dis00061.pdf
3. Mat-Shayuti, M. S., Zulkifli, H., Yahya, E., Othman, N. H., Hassan, Z. (2019). Development of Low-Cost, Non-Obtrusive Electrical Impedance Tomography Device for Liquid-Gas Flow Visualization. International Journal of Electrical and Electronic Engineering & Telecommunications, 119–126. doi: https://doi.org/10.18178/ijeetc.8.2.119-126
4. Meroni, D., Maglioli, C. C., Bovio, D., Greco, F. G., Aliverti, A. (2017). An electrical impedance tomography (EIT) multi-electrode needle-probe device for local assessment of heterogeneous tissue impeditivity. 2017 39th Annual International Conference of the IEEE Engineering in Medicine and Biology Society (EMBC). doi: https://doi.org/10.1109/embc.2017.8037091
5. Gschoßmann, S., Zhao, Y., Schagerl, M. (2016). Development of data acquisition devices for electrical impedance tomography of composite materials. 17th European Conference on Composite Materials, ECCM 2016. Munich, 126913.
6. S Arshad, S. H., Kunzika, J. S., Murphy, E. K., Odame, K., Halter, R. J. (2015). Towards a smart phone-based cardiac monitoring device using electrical impedance tomography. 2015 IEEE Biomedical Circuits and Systems Conference (BioCAS). doi: https://doi.org/10.1109/biocas.2015.7348452
7. Yao, A., Soleimani, M. (2012). A pressure mapping imaging device based on electrical impedance tomography of conductive fabrics. Sensor Review, 32 (4), 310–317. doi: https://doi.org/10.1108/02602281211257542

8. Deng, Q., Su, Y., Hu, S., Xiong, X., Juan, R., Zhang, Y., Ma, H. (2018). A Parallel Impedance Measurement System for Electrical Impedance Tomography System with Multi - Microcontroller - Unit Architecture. 2018 IEEE International Conference on Manipulation, Manufacturing and Measurement on the Nanoscale (3M-NANO). doi: https://doi.org/10.1109/3m-nano.2018.8552230
9. Menden, T., Orschulik, J., Tholen, T., Leonhardt, S., Walter, M. (2017). Approach to compensate measurement errors in electrical impedance tomography. 2017 IEEE Biomedical Circuits and Systems Conference (BioCAS). doi: https://doi.org/10.1109/biocas.2017.8325139
10. Gargiulo, G. D., Oh, T. I., Nguyen, D. T., Tapson, J., McEwan, A. L., Cohen, G. et. al. (2012). Active electrode design suitable for simultaneous EIT and EEG. Electronics Letters, 48 (25), 1583–1584. doi: https://doi.org/10.1049/el.2012.3212
11. Electrical impedance tomography. Available at: http://www.eit.org.uk/about.html
12. Kamenský, M., Kováč, K. (2011). Correction of ADC Errors by Additive Iterative Method with Dithering. Measurement Science Review, 11 (1). doi: https://doi.org/10.2478/v10048-011-0004-3
13. Troyanovskyi, V. M., Koldaev, V. D., Zapevalina, A. A., Serduk, O. A., Vasilchuk, K. S. (2017). Why the using of Nyquist-Shannon-Kotelnikov sampling theorem in real-time systems is not correct? 2017 IEEE Conference of Russian Young Researchers in Electrical and Electronic Engineering (EIConRus). doi: https://doi.org/10.1109/eiconrus.2017.7910736
14. Troyanovskyi, V. M., Koldaev, V. D., Zapevalina, A. A., Serduk, O. A., Vasilchuk, K. S. (2017). Why the using of Nyquist-Shannon-Kotelnikov sampling theorem in real-time systems is not correct? 2017 IEEE Conference of Russian Young Researchers in Electrical and Electronic Engineering (EIConRus). doi: https://doi.org/10.1109/eiconrus.2017.7910736
15. Ross, A. S., Saulnier, G. J., Newell, J. C., Isaacson, D. (2003). Current source design for electrical impedance tomography. Physiological Measurement, 24 (2), 509–516. doi: https://doi.org/10.1088/0967-3334/24/2/361
16. Micro CAP 12. Available at: http://www.spectrum-soft.com/index.shtm
17. 10 MHz, 20 V/μs, G = 1, 10, 100, 1000 iCMOS. Programmable Gain Instrumentation Amplifier. AD8253. Available at: https://www.analog.com/media/en/technical-documentation/data-sheets/AD8253.pdf